Journal of Sol-Gel Science and Technology (2020) 93:570–578
https://doi.org/10.1007/s10971-019-05085-1

ORIGINAL PAPER: SOL-GEL AND HYBRID MATERIALS FOR CATALYTIC, PHOTOELECTROCHEMICAL AND SENSOR APPLICATIONS

Check for updates

Photocatalytic activity and antibacterial behavior of TiO_2 coatings co-doped with copper and nitrogen via sol–gel method

Nasim Tahmasebizad[1] · Mohammad Taghi Hamedani[1] · Mehdi Shaban Ghazani[2] · Yaghoub Pazhuhanfar[3]

Received: 22 May 2019 / Accepted: 16 July 2019 / Published online: 12 August 2019

Abstract

The sol–gel process is used to prepare photocatalytic coatings with antibacterial properties. Also, doping with metallic or non-metallic elements has an impact on the antibacterial and photocatalytic activity of these coatings. Although there are many studies in this field, the effect of co-doping with Cu and N and their concentrations on the antibacterial properties of TiO_2 coatings against the *E. coli* and *S. aureus* bacteria has not been studied. In the present investigation, the sol–gel method was employed to deposit both undoped and Cu-N co-doped TiO_2 photocatalytic coatings on glass surface, which are expected to degrade bacterial and chemical contaminants in water while exposed to visible sunlight wavelengths. Before the coating process, an appropriate heat treatment was applied on the samples and the quality of coatings, band gap energy, and also photocatalytic and antibacterial properties were evaluated. Results showed that, in the presence of dopants, the band gap become narrower and the absorption spectrum is transferred from the ultraviolet to the visible light range. Also, it was demonstrated that, under the visible light radiation, all of the co-doped samples show higher photocatalytic activity than the undoped ones. Meanwhile, the antibacterial characteristics of TiO_2 coatings was enhanced by increasing the dopant concentration when exposing to sunlight.

Graphical Abstract

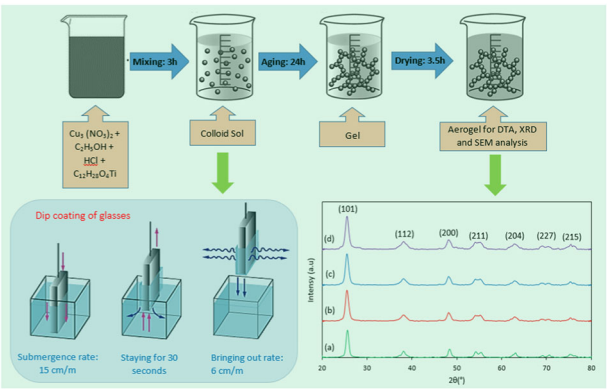

✉ Mehdi Shaban Ghazani
m_shaban@bonabu.ac.ir

[1] Department of Materials Science Engineering, Faculty of Mechanical Engineering, University of Tabriz, P.O. Box 51666-16471, Tabriz, Iran

[2] Department of Materials Science Engineering, University of Bonab, P.O. Box 5551761167, Bonab, Iran

[3] Department of Materials Science Engineering, Sahand University of Technology, P.O. Box 51335-1996, Tabriz, Iran

Highlights

- TiO_2 coatings co-doped with different concentrations of copper and nitrogen were applied on glass surface using sol–gel process.
- The influence of the dopant concentration on the photocatalytic activity and antibacterial properties was discussed.
- Under the visible light radiation, all of the co-doped samples have higher photocatalytic activities than the undoped ones, while the 0.75%Cu-N sample has the best photocatalytic activity, even better than the 1% Cu-N one.

Keywords Titanium dioxide · Co-doping · Sol–gel method · Band gap · Photocatalyric activity

1 Introduction

In the 1980s, the process named as solar disinfection (SODIS) was expanded to disinfect water in the most convenient and inexpensive way [1, 2]. Later in 1991, the Swiss Federal Institute for Environmental Science and Technology funded a project to evaluate SODIS as a solution to eliminate the household water impurities and to avoid diarrhea especially in developing countries [3]. It was recommended to expose bottles of water to sun waves for 6 h in sunny or 2 days in cloudy days. Illness-causing organisms would be deactivated as a result of ultraviolet (UV) light, thermal inactivation, and photo-oxidative destruction by this method [4, 5]. The photocatalytic activity of silver nanoparticles was investigated by Memon and his coworkers [6]. They indicated that the synthesized silver nanoparticles with and without the presence of sunlight demonstrates significant antimicrobial activities. They also suggested that the green synthesis of Ag nanoparticles can be alternative to the chemical methods and suitable for developing an easy process industrial production. Other similar works were also conducted by Memon and his coworkers regarding the photocatalytic activity and antimicrobial properties of different engineering materials [7–9]. The oxidizing effect of photo-generated holes in TiO_2 combined with its low price and relative physical and chemical stability make it a desirable option to be used in a plenty of applications such as a photocatalyst where degrading the organic pollutants into more eco-friendly chemical species occurs. Hence, TiO_2 is considered as a high-potential photocatalyst for water and air purification in addition to self-cleaning surfaces [10]. Besides, thanks to its high oxidation activity and superhydrophilicity, it can be used as an antibacterial agent [11].

According to previous findings, undoped TiO_2 photocatalysts has shown relatively high photo-reactivity and self-sterilization properties under UV radiation. Moreover, it is desired to apply photocatalysts with high quantum yields under visible (Vis) light (>400 nm) in order to be able to trap the rest of the solar spectrum and obtain more efficient chemical contaminant degradation. A possible solution could be the doping of TiO_2 nanostructures to reach better photocatalytic properties under the sunlight. Doping TiO_2 would lead to higher photocatalytic properties if it could be applied on the surface with metals and/or nonmetal elements [12–14]. The increment on the surface-to-volume ratio in nanostructured layers results in higher reactive surface. Therefore, the surface adsorption and interfacial redox reactions can be empowered by applying nanostructured semiconductor coatings [15]. Substitution doping plays an important role to reduce the band gap of TiO_2 nanostructures and to absorb the higher fraction of solar radiation. Compositional doping is introduced to narrow the TiO_2 band gap. Considering the crystal structure of TiO_2, it seems that replacement of Ti^{4+} with any cation is easier than to substitute O^{2-} with any other anion due to the charge states and ionic radii difference [16, 17]. To exemplify the nonmetal doping of TiO_2 in anionic sites, doping by anionic species (N, S, C, B, P, I, or F) have been done [18, 19]. More precise calculations demonstrate the band-gap narrowing, which derives from the electronic perturbations caused by the deformation of lattice parameters and/or by the presence of the trap states within conduction and valence bands of TiO_2 [20, 21].

A wide range of procedures has been applied till now to introduce the dopants in TiO_2 structure, namely, by wet-chemical, electrochemical, and physical methods [22, 23]. In this regard, sol–gel is one of the most practical ways; it is used mainly to produce thin films and powder catalysts. Many studies revealed that different variants and modifications of the process can be used to produce pure thin films or powders in large homogeneous concentration. The process involves conversion of monomers into a colloidal solution (sol) that acts as the precursor for an integrated network (or gel) of either discrete particles or network polymers.

It was demonstrated that Co-doped TiO_2 thin films show enhanced antibacterial properties compared with single doped coatings. Ashkarran et al. [24] investigated the effect of silver and nitrogen doping on the antibacterial properties of TiO_2 nanoparticles synthesized by sol–gel method and showed that the silver- and nitrogen-doped TiO_2 nanoparticles extend the light absorption spectrum toward the Vis region and enhance the photo-degradation effect and bacteria inactivation efficiency of the nanoparticles under the Vis light irradiation. Their work demonstrated that the

double doped TiO_2 nanoparticles exhibit highest photocatalytic and antibacterial activity compared with single doped nanoparticles. Yuan et al. [25] reported similar results and concluded that both Ag- and N-doped TiO_2 could increase the antibacterial properties of TiO_2 nanoparticles under fluorescent light irradiation while the 1% Ag–N–TiO_2 has the highest antibacterial activity. Wang et al. [26] studied the antibacterial activity of yttrium- and zinc-doped TiO_2 and revealed that co-doped samples exhibit better performance than zinc- and yttrium-doped alone under Vis light irradiation.

This paper aims to study the ability of nitrogen and copper co-doped TiO_2 thin films, which were applied on soda lime glass surface by sol–gel process, to enhance the sunlight-mediated degradation of indicator bacteria colonies in water. In order to enhance either photocatalytic or antibacterial properties of TiO_2 nanoparticles, in the present work we prepared double doped TiO_2 with copper and nitrogen. We have investigated the effect of different concentration of dopants on the photocatalytic activities and antibacterial properties of the produced nanoparticles under Vis light and UV irradiation. Furthermore, the optimum amount of copper and nitrogen dopants was determined. For this reason, after preparation of TiO_2 coatings using sol–gel method, the different characteristics of coatings such as antibacterial properties, photocatalytic activity, the present phases, and crystallite sizes were evaluated.

2 Experimental

2.1 Coating procedure

In this study SiO_2 thin film, as an adhesive sublayer, was deposited on the glass surface by sol–gel method using a tetra-urethous silicate and ethanol solution, which was homogenized by a magnetic stirrer for 3 h. In order to apply undoped TiO_2 coating, the required sol, including tetrazinopropyl orutylateate dissolved in ethanol and chloridric acid as a catalyst, was prepared with a weight ratio of 1/30/1, respectively. For the main coating process, tetra-isopropyl ortho-titanate ($C_{12}H_{28}O_4Ti$, as a titania precursor), tetrahydroethyl octosilicate ($C_8H_{20}O_4Si$, as a SiO_2 precursor), copper nitrate (Cu_3 $(NO_3)_2$, as a nitrogen precursor), and urea (CH_4N_2O, as a copper precursor) were used with 98% purity. The solvent was ethanol with 99.6% purity and the applied catalyst was HCl. Copper and nitrogen doping of the sols was achieved using copper nitrate and urea as dopant precursors. To synthesize N-Cu-TiO_2, tetraezopropyl ortho-ethyl acetate, ethanol, and hydrochloric acid were weighed with 1/35/1 ratio. Then the precise amounts of copper nitrate and urea with different values (0.5, 1, and 1.5 wt% of TiO_2) were measured. Finally, half of the measured amount of ethanol was mixed with tetra-isopropyl ortho-titanate and hydrochloric acid, which was stirred and homogenized for 30 min by a magnetic stirrer (solution A). Half of the ethanol residue was mixed with copper nitrate and urea and dissolved with a magnetic stirrer for half an hour (solution B). Then solution A was added to this solution drop by drop and allowed to dissolve for a period of 3 h in the stirrer. Finally, the coatings were applied on the glass surface after keeping the prepared sol at room temperature for 24 h. After washing the glass slides in water and ethanol and air drying, the samples were inserted in the sol at the rate of 15 cm/min for 30 s after which taken out at the rate of 6 cm/min.

2.2 Differential thermal analysis (DTA)

To evaluate the thermal behavior of coatings and determination of the appropriate heat treatment temperatures, DTA analysis was performed using the DTG-66AH-SHIMADZU device. Thermal analysis of TiO_2 powder was conducted at a heating rate of 10 °C/min. The reference material was α-alumina and the temperature increasing rate was set as 10 °C/min. To provide TiO_2 powder, the prepared sols were exposed to free air at ambient temperature for 3 days to form a gel. Then the gels got dried at 100 °C for 24 h and finally grinded into powder. The appropriate heat treatment, to achieve the desired crystalline phase in the coatings, was performed for 2 h in an electric furnace at the maximum crystallization temperature determined by DTA.

2.3 X-ray diffraction (XRD) analysis

To identify the different phases in the heat-treated samples, The XRD patterns were acquired by Siemens D500 diffractometer. Identification of the phases was performed with a PDF-card of each phase, employing the XPert HighScore software. The crystallite size was measured using the Sherer's equation as below [17, 27]:

$$D = 0.9\lambda/B\cos\theta_B \quad (1)$$

where D is the crystallite size, B is the peak width in half of the maximum intensity (radian), λ is the X-ray wavelength, and θ_B is the Brag angle corresponding to the diffraction peak.

2.4 Field emission scanning electron microscopic (FE-SEM) characterization

FESEM (MIRA3 TESCAN) was used for microstructural characterization of undoped and co-doped TiO_2 coatings. It was operated at an accelerating voltage of 30 kV and working distance of 5 mm.

2.5 UV-Vis spectroscopy

To assess the absorption edge and band gap of titania coatings, the samples were exposed to UV-Vis test using the Spectrophotometer$_{35}$ and the following equation was employed [27, 28]:

$$E_{bg} = \frac{1240}{\lambda} \quad (2)$$

where λ is the wavelength (nm) and E_{bg} is the band gap energy (eV).

2.6 Photocatalytic property assessment

The photocatalytic property of the coatings was studied by methylene blue ($C_{16}H_{18}N_3SCl$) degradation (5 mg/l) in the presence of sunlight (using methane halide lamp) and UV radiation (using UV-c Philips, 1.5 W lamp). The test duration was 30, 60, 90, 120, 150, and 180 min after which the relevant concentrations were calculated by a spectrophotometer. By drawing the C/C_0 curves as a function of time, the amounts of removed colors caused by the photocatalytic activity of the coatings could be comparable [29]:

$$\log\left(\frac{I}{I_0}\right) = \varepsilon.C.b \quad (3)$$

In the above equation, ε is the molar absorption capability, C is the methylene blue sample concentration, b is the sample length exposed to radiation, I is the transition intensity, and I_0 is the initial radiation intensity.

2.7 Antibacterial trials and calculations

Antibacterial examinations were done on two representatives of each type of bacteria including *Escherichia coli* (AT-CC 25922) in Gram-negative category and *Staphylococcus aureus* (AT-CC 33591) in the Gram-positive group. The Luria Broth (LB) solution was prepared by dissolving 17 g of this powder in 500 cc of deionized water. The number of bacterial colonies was enumerated by the standard plate count techniques (15 cc in each plate). Plates were incubated at 37 °C for 24 h prior to enumeration. The mixture of nutrient broth (1.3 g) well mixed in deionized water (100 cc) was prepared in the same way as LB medium. The solution was autoclaved at 120 °C for 15 min, and then the bacteria prepared in the previous steps were transferred to this medium and incubated at 37 °C for 18 h, till the solvent color got dark. In order to dilute the final solution, the bacteria were inserted in 250 ml of the physiological saline. To be able to compare and verify the results, specimens were exposed to natural sunlight for 2 h from 12 to 2 p.m. with an average ambient temperature of 30 °C. The UV radiation level was 9 (very high) and the sky was all clear during the whole test time. The specimens were then incubated for 24 h and finally bacterial colonies were enumerated to plot the relative activity graphs. To determine the surface activity level against the bacteria growth, the relative activity was plotted as a function of dopant concentrations [30, 31]:

$$\text{Relative activity} = \{\log(A/B)/\log(A)\} \times 100 \quad (4)$$

$$\text{Antibacterial activity} = \log(A/B) \quad (5)$$

where A and B are the number of bacterial colonies on the surface of the coated samples and the reference surface, respectively. If Ra = 100, the surface is completely antibacterial, whereas Ra = 0 shows no antibacterial activity [31].

2.8 Glass sample preparation

In order to prepare the glass samples, they were autoclaved at 120 °C. Then the bacteria solution was injected by a sampler on the glass surface (100 ml for each sample). Finally, they were exposed to natural sunlight and methane halide lamp with a similar spectrum, every 2 h, periodically. Before counting the numbers of colonies, the specimens were incubated for 24 h.

3 Results and Discussion

According to the DTA graphs represented in Fig. 1, it is obvious that, by increasing the Cu-N dopant concentration, the titania phase evolution temperature declines from 415 °C in 0.5% Cu-N to 395 °C in 1% Cu-N. This temperature is about 480 °C in undoped samples (Table 1). So, by adding 0.5% dopants to titania, a big fall in crystallization temperature occurs, but by increasing the dopant concentration from 0.5% to 1% this change is not very significant. Considering the XRD patterns shown in Fig. 2, it is deduced that the only present phase in the coatings is anatase. Moreover, by increasing the dopant's concentration, the intensity of XRD peaks increases. Comparing the coating grain sizes obtained by Sherer's equation, it is concluded that the grain size is decreased by increasing the dopant concentration in the coating. The reason could rely on the blocking role of dopants during the grain growth in titania structure. Dopants' ions can substitute titanium and oxygen ions in the structure of titania and consequently cause a tensile stress, which could block the grain growth. Moreover, dopants can prevent the loss of anatase phase and its transformation into the rutile phase (according to XRD patterns). SEM micrographs of undoped and 1% Cu-N-doped samples clearly confirm the grain size reduction in co-doped coatings (Fig. 3).

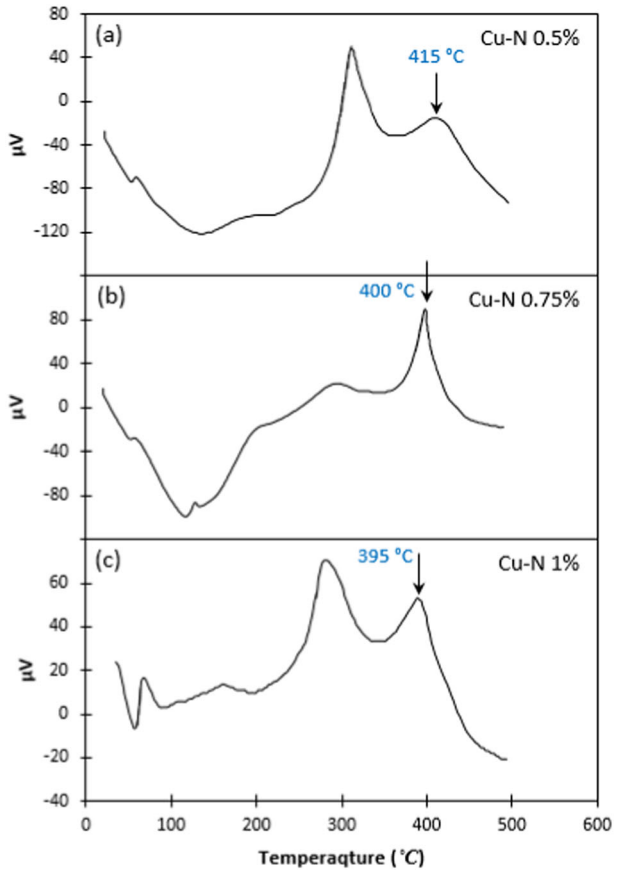

Fig. 1 Differential thermal analysis graphs in the Cu-N co-doped samples with different percentages of dopants: **a** 0.5% Cu-N, **b** 0.75% Cu-N, and **c** 1% Cu-N

Table. 1 The crystallization temperature in different Cu/N-doped samples

Sample	Crystallization temperature (°C)	Wave length (nm)	Band gap energy (eV)
TiO_2	480	372	3.33
TiO_2–0.5% Cu/N	415	437	2.86
TiO_2–0.75% Cu/N	400	445	2.81
TiO_2–1% Cu/N	395	447	2.77

The UV-Vis absorption spectrum for TiO_2 pure film and co-doped coatings containing 0.5, 0.75, and 1% dopants are shown in Fig. 4. In order to have more precise examination on the band gap energy, the tangent line on the absorption diagrams as a function of wavelength is plotted at the absorption edge (Fig. 4). The first achieved result is that, in the presence of dopants, the absorption spectrum is transferred from the UV to the Vis light range (wave lengths >372 nm). The second fact is that, by increasing the dopants' value, the band gap energy is reduced, so the band gap becomes narrower (Table 1). The reason is the creation of a subsidiary quantum level by dopant ions at the bottom

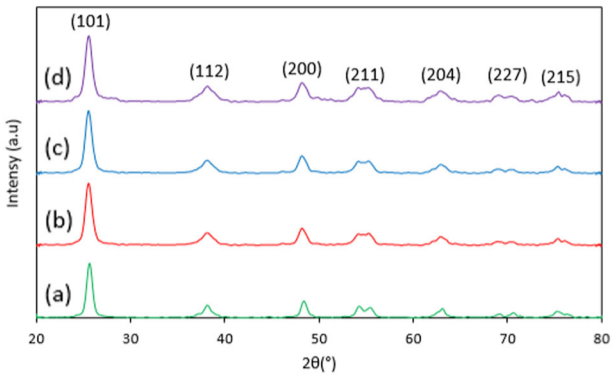

Fig. 2 The X-ray diffraction patterns for TiO_2 pure film **a** and co-doped coatings containing 0.5% **b**, 0.75% **c** and 1% **d** of Cu/N

of the conduction band and above the valence band in the titania structure. As a result, the relevant gap between the valence band and the conduction band and consequently the band gap energy is decreased.

To investigate the expected photocatalytic property improvement, the undoped sample and Cu-N co-doped samples were all exposed to UV and Vis light radiation. By drawing the C/C_0 as a function of time (as explained before), the amounts of removed colors caused by the photocatalytic activity of the coatings were obtained in different test durations. According to Fig. 5a, it is detected that, under the Vis light radiation, all of the co-doped samples show better photocatalytic activities than the undoped one, since the C value decreases with co-doping of TiO_2 coating with N and Cu atoms. Amazingly the 0.75% Cu-N sample has the best photocatalytic property, even better than the 1% Cu-N one. So a constant decreasing trend cannot be defined for this property. The suggested reason is that, by doping the coatings, the band gap gets narrower and the grain size becomes smaller, so the expected result is the improvement of photocatalytic activity. Meanwhile, in 1% Cu-N sample, the recombination of electron–hole couples may speed up, which leads to lowering the photocatalytic activity. On the other hand, owing to shifting the absorption edge of co-doped sample to Vis region, the adverse trend occurs in the samples exposed to UV waves. It means that the co-doped samples show weaker photocatalytic activity compared to the undoped one (Fig. 5b). Among all of the tested coatings, 0.5% Cu-N shows the best photocatalytic activity, which comes from its closest band gap energy to UV region.

In a series of antibacterial property examinations, after enumerating the numbers of bacterial colonies (*S. aureus* and *E. coli*) exposed to methane halide for 2 h and then incubated for 24 h, the results were plotted as diagrams. Examining the *S. aureus* diagram, the results obtained for samples exposed to methane halide (Fig. 6a) confirm the previously achieved results in photocatalytic activity tests in

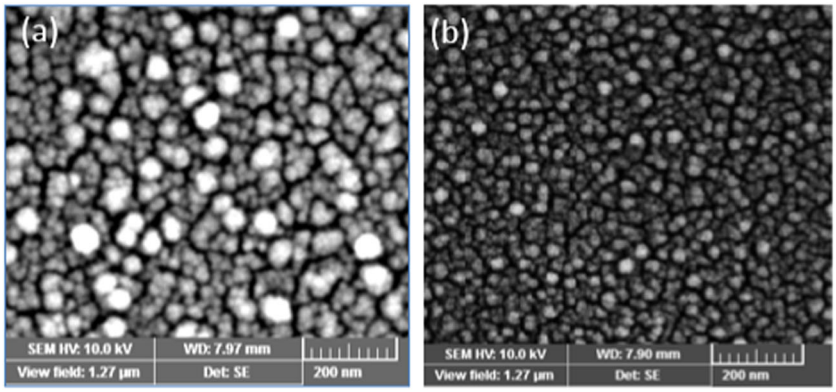

Fig. 3 Scanning electron microscopic microstructure of undoped **a** and 1% Cu-N-doped **b** TiO_2 coating applied at 500 °C using sol–gel method

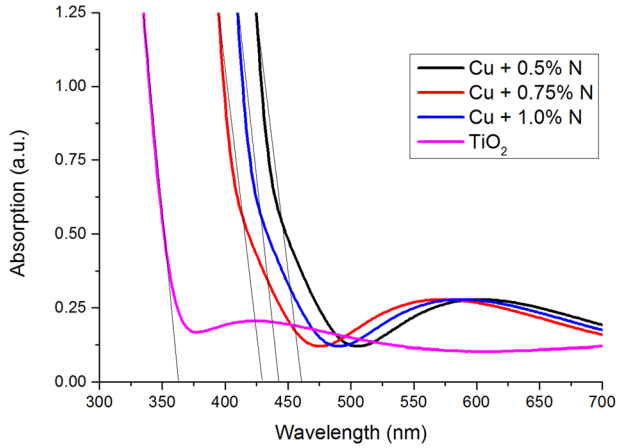

Fig. 4 The ultraviolet–visible absorption spectrum for TiO_2 pure film and co-doped coatings containing 0.5, 0.75 and 1% dopants

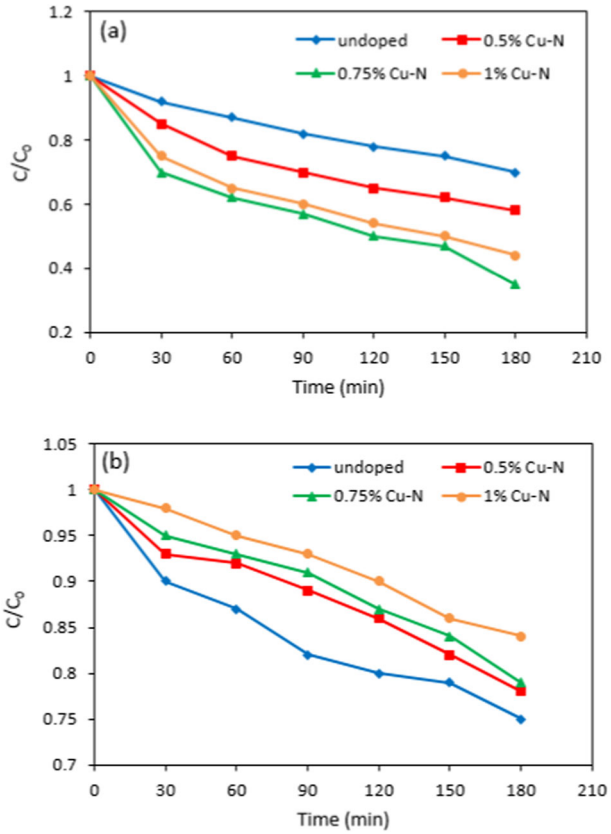

Fig. 5 Photocatalytic activity results in undoped and different co-doped samples exposed to visible light **a** and ultraviolet radiation **b**

which 0.75% Cu-N coating shows the highest quality, while this trend is not seen in *E. coli* bacterial colonies (Fig. 6b). It means that, by increasing the dopants' concentration, the relative activity in *E. coli* medium increases constantly. Also a small jump could be seen when switching from 0.75% Cu-N to 1% Cu-N point. In order to recheck the obtained results for *S. aureus* bacteria, once again the test has been done under the direct natural sunlight. The specimens were exposed to sunlight for 2 h from 12 to 2 p.m. with an average ambient temperature of 30 °C. The UV radiation level was 9 (very high) and the sky was all clear during the whole test time. The specimens were then incubated for 24 h and finally bacterial colonies were enumerated to plot the relative activity graphs. As is seen in Fig. 6c, although the increasing trend was obvious, there was not much difference between the 0.75% Cu-N and 1% Cu-N points (the specimens of grown *S. aureus* bacteria are shown in Figs. 7 and 8). The suggested mechanism to describe the antibacterial behavior is as below: the outer membrane of some bacterial structure is surrounded by a hydrocarbonate gelatinous layer, which protects the bacteria from environmental attacks to keep its pathogenic potential. If the bacteria lose this layer, it becomes harmless and acts like normal hydrocarbon contaminations in the air. While exposed to sunlight, the protective layer weakens and its molecular bonds get looser, so the bacterial colonies get disordered. Over time, the bond is completely broken, and the protective layer and membrane structure totally get destroyed. Finally, it is worth to note that photocatalytic oxidation, which generate superoxide (O_2^-) and hydroxide radical (OH^-), could be harmful for human physiological system. Also, the use of titanium dioxide (TiO_2) nanoparticles has been reported to have led to pregnancy

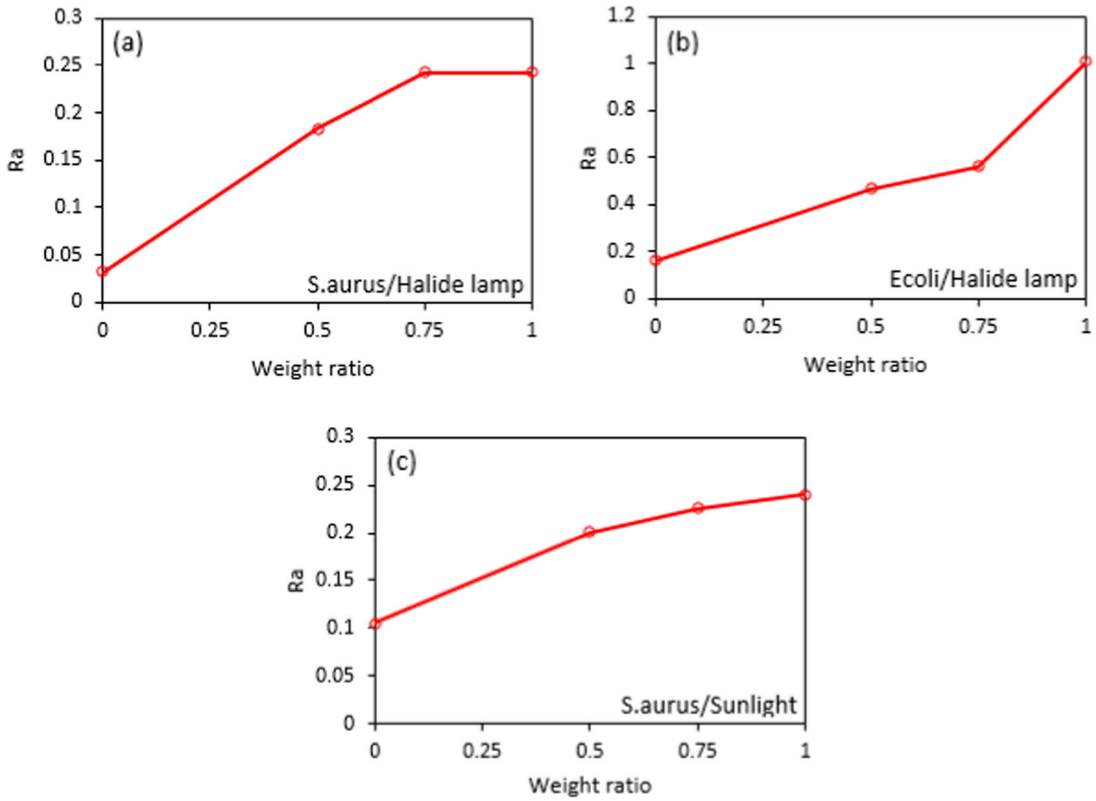

Fig. 6 Relative antibacterial activity of samples with different dopants concentrations in *S. aureus* medium **a** and *E. coli* medium **b** exposing to methane halide lamp radiation and in *S. aureus* medium exposing to sunlight **c**

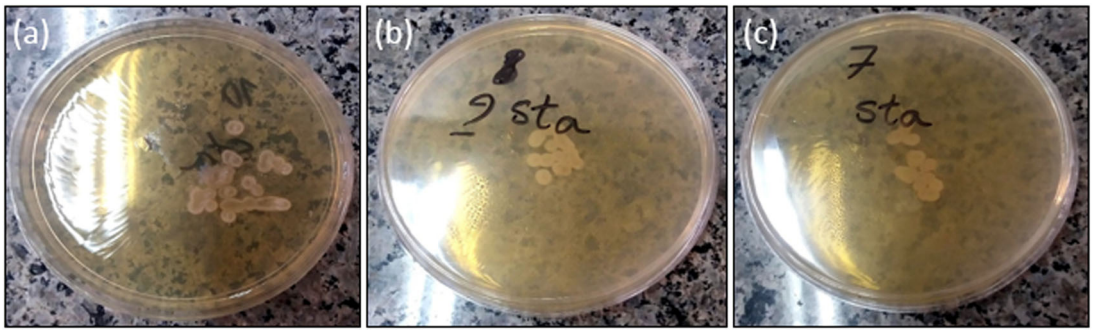

Fig. 7 The *S. aureus* medium after exposing to methane halide lamp radiation: **a** the uncoated sample, **b** the undoped coating and **c** the 0.75% Cu-N-doped coated sample

complications in mice and neurotoxicity in their offspring. Therefore, urgent evaluation of nanoparticles and their risk to human health is important, particularly in cosmetic and industrial areas where materials such as titanium dioxide are in regular use [32, 33]. There are methods for improving the performance and reducing toxicity of nanoparticles in medical design, such as biocompatible-coating materials or biodegradable/biocompatible nanoparticles. Most metal oxide nanoparticles show toxic effects, but no toxic effects have been observed with biocompatible coatings [34].

4 Conclusions

In the present investigation, nitrogen and copper in three different concentrations were co-doped in titania structure to improve the photocatalytic properties of the coatings applied by sol–gel method on glass surface. The main results can be summarized as below:

– Assuming DTA graphs, increasing the Cu-N concentration reduces the titania phase evolution temperature

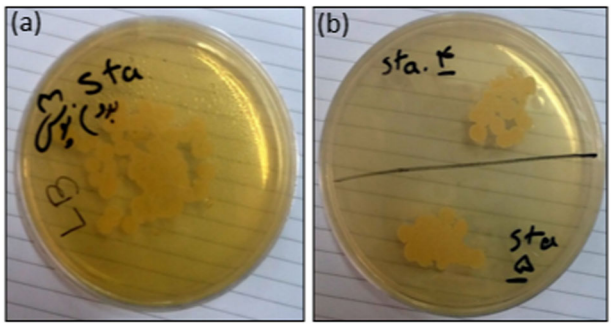

Fig. 8 The *S. aureus* medium after exposing to sunlight: **a** the uncoated sample, **b** the 0.75% Cu-N-doped coated sample on the top and 1% Cu-N-doped coated sample on the bottom

from 415 °C in 0.5% Cu-N to 395 °C in 1% Cu-N, while the phase evolution temperature is 480 °C in undoped samples. It means that by adding 0.5% dopants to titania we would have a big fall in crystallization temperature, meanwhile by increasing the dopant concentration (from 0.5% to 1%), this change is not very significant.

- By evaluating the XRD patterns, the only detected phase in the coatings is anatase. Moreover, the grain size decreases with increasing the dopant concentration.
- Comparing the band gap energies shows that, in the presence of dopants, the absorption spectrum is transferred from the UV to the Vis light range, and by increasing the dopants value, the band gap energy is reduced, so the band gap becomes narrower.
- Considering the C/C_0 vs. time graphs, it is concluded that, under the Vis light radiation, all of the co-doped samples have higher photocatalytic activities than the undoped one, while the 0.75%Cu-N sample has the best photocatalytic activity, even better than the 1% Cu-N one. However, the adverse trend occurs in samples exposed to UV waves.
- The number of colonies in samples exposed to the radiation of methane halide lamp confirms the obtained results of photocatalytic tests, in which 0.75% Cu-N coating shows the highest quality. However, this trend is not observed in *E. coli* bacteria colonies.

Compliance with ethical standards

Conflict of interest The authors declare that they have no conflict of interest.

Ethical standards This work complies with the ethical rules of this journal.

Publisher's note: Springer Nature remains neutral with regard to jurisdictional claims in published maps and institutional affiliations.

References

1. Byrne JA, Fernandez-Ibanez PA, Dunlop PS, Alrousan D, Hamilton JW (2011) Photocatalytic enhancement for solar disinfection of water: a review. Int J Photoenergy 2011:798051
2. Caslake LF, Connolly DJ, Menon V, Duncanson CM, Rojas R, Tavakoli J (2004) Disinfection of contaminated water by using solar irradiation. Appl Environ Microbiol 70(2):1145–1151
3. Parsons JJC (2002) Evaluating solar disinfection for point-of-use water treatment in non-tropical climates. Massachusetts Institute of Technology, Harvard, MA
4. Pattison DI, Rahmanto AS, Davies MJ (2012) Photo-oxidation of proteins. Photochem Photobiol Sci 11(1):38–53
5. Rule Wigginton K, Menin L, Montoya JP, Kohn T (2010) Oxidation of virus proteins during UV254 and singlet oxygen mediated inactivation. Environ Sci Technol 44(14):5437–5443
6. Liu Y, Hussain M, Memon H, Yasin S (2015) Solar irradiation and nageia nagi extract assisted rapid synthesis of silver nanoparticles and their antibacterial activity. Dig J Nanomater Biostructure 10(3):1019–1024
7. Memon H, Wang H, Yasin S, Halepoto A (2018) Influence of incorporating silver nanoparticles in protease treatment on fiber friction, antistatic and antibacterial properties of wool fibers, J Chem 2018:4845687. https://doi.org/10.1155/2018/4845687
8. Memon H, Kumari N, Jatoi AW, Khoso NA (2016) Study of the indoor decontamination using nanocoated woven polyester fabric. Int Nano Lett 7(1):1–7
9. Memon H, Kumari N (2016) Study of multifunctional nanocoated cold plasma treated polyester cotton blended curtains. Surf Rev Lett 23(5):1–11
10. Guan K (2005) Relationship between photocatalytic activity, hydrophilicity and self-cleaning effect of TiO_2/SiO_2 films. Surf Coat Technol 191(2–3):155–160
11. Yu JC, Ho W, Lin J, Yip H, Wong PK (2003) Photocatalytic activity, antibacterial effect, and photoinduced hydrophilicity of TiO_2 films coated on a stainless steel substrate. Environ Sci Technol 37(10):2296–2301
12. Li J, Wang D, Liu H, Zhu Z (2012) Multilayered Mo-doped TiO_2 nanofibers and enhanced photocatalytic activity. Mater Manuf Process 27(6):631–635
13. Sakthivel S, Kisch H (2003) Photocatalytic and photoelectrochemical properties of nitrogen-doped titanium dioxide. Chem Phys Chem 4(5):487–490
14. Songara S, Patra M, Manoth M, Saini L, Gupta V, Gowd G, Vadera S, Kumar N (2010) Synthesis and studies on photochromic properties of vanadium doped TiO_2 nanoparticles. J Photochem Photobiol A Chem 209(1):68–73
15. Shankar K, Basham JI, Allam NK, Varghese OK, Mor GK, Feng X, Paulose M, Seabold JA, Choi K-S, Grimes CA (2009) Recent advances in the use of TiO_2 nanotube and nanowire arrays for oxidative photoelectrochemistry. J Phys Chem C 113 (16):6327–6359
16. Dvoranova D, Brezova V, Mazúr M, Malati MA (2002) Investigations of metal-doped titanium dioxide photocatalysts. Appl Catal B Environ 37(2):91–105
17. Wang Y, Hao Y, Cheng H, Ma J, Xu B, Li W, Cai S (1999) The photoelectrochemistry of transition metal-ion-doped TiO_2 nanocrystalline electrodes and higher solar cell conversion efficiency based on Zn2+-doped TiO_2 electrode. J Mater Sci 34 (12):2773–2779
18. Burda C, Lou Y, Chen X, Samia AC, Stout J, Gole JL (2003) Enhanced nitrogen doping in TiO_2 nanoparticles. Nano Lett 3 (8):1049–1051
19. Kim S-W, Khan R, Kim T-J, Kim W-J (2008) Synthesis, characterization, and application of Zr, S Co-doped TiO_2 as visible-

light active photocatalyst. Bull Korean Chem Soc 29 (6):1217–1223
20. Serpone N (2006) Is the band gap of pristine TiO_2 narrowed by anion-and cation-doping of titanium dioxide in second-generation photocatalysts? ACS Publications, Washington
21. Wang H, Lewis J (2005) Second-generation photocatalytic materials: anion-doped TiO_2. J Phys Condens Matter 18(2):421
22. Diwald O, Thompson TL, Goralski EG, Walck SD, Yates JT (2004) The effect of nitrogen ion implantation on the photoactivity of TiO_2 rutile single crystals. J Phys Chem B 108(1):52–57
23. Sakthivel S, Janczarek M, Kisch H (2004) Visible light activity and photoelectrochemical properties of nitrogen-doped TiO_2. J Phys Chem B 108(50):19384–19387
24. Ashkarran AA, Hamidinezhad H, Haddadi H, Mahmoudi M (2014) Double-doped TiO_2 nanoparticles as an efficient visible-light-active photocatalyst and antibacterial agent under solar simulated light. Appl Surf Sci 301:338–345
25. Yuan Y, Ding J, Xu J, Deng J, Guo J (2010) TiO_2 nanoparticles co-doped with silver and nitrogen for antibacterial application. J Nanosci Nanotechnol 10:4868–4874
26. Wang Y, Yang H, Xue X (2014) Synergistic antibacterial activity of TiO_2 co-doped with zinc and yittrium. Vacuum 107:28–32
27. Mahmood Q, Afzal A, Siddiqi HM, Habib A (2013) Sol–gel synthesis of tetragonal ZrO_2 nanoparticles stabilized by crystallite size and oxygen vacancies. J Sol-Gel Sci Technol 67 (3):670–674
28. Suwanboon S, Amornpitoksuk P, Sukolrat A (2011) Dependence of optical properties on doping metal, crystallite size and defect concentration of M-doped ZnO nanopowders (M= Al, Mg, Ti). Ceram Int 37(4):1359–1365
29. Kurniawan C (2016) Spectroelectrochemical study of electron transfer steps at ITO electrode modified by molecular layer with viologen moieties with and without Pt complexes, PhD thesis, Hokkaido University
30. Fisher MB, Keane DA, Fernandez-Ibanez P, Colreavy J, Hinder SJ, McGuigan KG, Pillai SC (2013) Nitrogen and copper doped solar light active TiO_2 photocatalysts for water decontamination. Appl Catal B Environ 130:8–13
31. Mungkalasiri J, Bedel L, Emieux F, Vettese-Di Cara A, Freney J, Maury F, Renaud FN (2014) Antibacterial properties of TiO_2–Cu composite thin films grown by a one step DLICVD process. Surf Coat Technol 242:187–194
32. Memon H, Yasin S, Khoso NA, Hussain M (2015) Indoor decontamination textiles by photocatalytic oxidation: a review. J Nanotechnol 2015:104142. https://doi.org/10.1155/2015/104142
33. Yamashita K, Yoshioka Y, Higashisaka K et al. (2015) Silica and titanium dioxide nanoparticles cause pregnancy complications in mice. Nat Nanotechnol 6(5):321–328
34. Ai J, Biazar E, Jafrpour M, Montazeri M, Majdi A, Aminifard S, Zafari M, Akbari HR, Rad HG (2011) Nanotoxicology and nanoparticle safety in biomedical designs. Int J Nanomed 6:1117–1127